Pure & Appl. Chem., Vol. 67, No. 4, pp. 527–534, 1995.
Printed in Great Britain.

Chemical association model for supercritical fluid solvents: Application to fluid compressibility isotherms well above the critical region for methane, 360–470 K, 0–1000 MPa

F. W. Getzen

Chemistry Department, N. C. State University,
Raleigh, North Carolina, U SA

Abstract: Solvent properties of supercritical fluid depend upon their molecular physical dimensions and the extent of their molecular interactions. The nonideality of fluids in the supercritical region, to some extent, can be attributed to molecular associations which, in turn, affect solubility behavior. An association model in terms of cluster formation is developed to explain fluid compressibility behavior far above the supercritical region. The development incorporates a continuous specie association together with mass balance to provide agreement with observed gas compressibility behavior. This approach incorporates two general characteristics of gas isothermal compressibility, large values at low pressures and small values at high pressures, into a simple two specie system which can account for fluid P-V-T behavior over wide ranges of temperature and pressure in the supercritical regions where such fluids find practical uses as solvents in certain commercial applications. Excellent agreement is obtained using reported compressibility data for methane in the ranges of 360-470 K and 0-1000 MPa.

INTRODUCTION

Supercritical fluids are becoming increasingly more useful as industrial solvents with the development of reactors which can operate at extreme pressure and temperature conditions. A knowledge of the physical and chemical nature of the supercritical fluid solvents is essential for the most efficient use of such materials in commercial applications. To the extent possible, it is essential to know the nature and physical makeup of the solvent systems at the microscopic level for the utilization of the solvent properties of supercritical fluids to their greatest advantage.

Of considerable significance for the understanding of the nature of supercritical fluids is the description of P-V-T behavior throughout the supercritical region. Progressive development in this area has focused upon equations of state which provide good data fits for fluid density versus pressure and temperature over extreme ranges with the introduction of increasing numbers of virial coefficients and smoothing parameters. For the most part,

classical developments have relied heavily upon van der Waal's excluded volumes and interaction potential energies to account for gas imperfections. With the exceptions for known chemical reactions, chemical associations and cluster formations have not been invoked extensively to explain P-V-T behavior over wide ranges of conditions. Even so, as this development demonstrates, the successive clustering of molecular species with increasing pressure when combined with clearly defined excluded volume terms can successfully describe observed P-V-T behavior over wide ranges of temperature and pressure in the supercritical region.

This clustering model is based principally upon the classical successive associations of the type involved in many typical polymerization reactions. To account for total conservation of volume, the system volume is assumed to be represented by the hard sphere volume of the individual particles, the free (gas) volume associated with the point (monomer) masses in random translational motion, and the additional excluded volume provided in the framework of the associated particle clusters. In this basic approach, only the monomers are associated with the free volume and only the associated clusters are assumed to contribute to the excluded volume. Both the monomers and the associated species retain their appropriate hard sphere volumes.

MODEL DEVELOPMENT

The molecular species are assumed to undergo successive reactions of the type represented by a typical Flory reaction mode as indicated in equation (1)

$$A_1 + A_i = A_{i+1} \qquad i = 1, 2, \ldots \qquad (1)$$

for which, with x's representing mole fractions

$$K = K_o P = \left(\frac{x_{i+1}}{x_i x_1} \right) , \quad i = 1, 2, \ldots \qquad (2)$$

From mass balance, one obtains

$$(n_t / n_o) = 1/(1 + K)$$

$$(n_x / n_t) = x = 1/(1 + K)$$

$$and \quad (n_c / n_t) = (1 - x) = K/(1 + K) \qquad (3)$$

From the general equation of state for gases (supercritical fluids), as a function of pressure

$$(PV / RT) = Z = 1 + BP + CP^2 + \ldots . \qquad (4)$$

one obtains

$$Z = bP / RT + (n_x / n_o) + (n_c / n_o) V_c P / RT \qquad (5)$$

so that

$$(Z - bP / RT) = x^2 + x(1 - x) V_c P / RT \qquad (6)$$

wherein V_c is associated species excluded volume as given by

$$V_c = v_o + v_1(1 - x) = v_o + v_1 K_o P / (1 + K_o P) \qquad (7)$$

Incorporating the second virial coefficient, B, and using equation (7), equation (6) becomes

$$(Z - BP/RT) = f(P) = 2K_o P + 1/(1 + K_o P)^2 +$$
$$(v_o + v_1 K_o P/(1 + K_o P))K_o P^2/(RT(1 + K_o P)^2) \qquad (8)$$

Equation (8) was used as the regression equation with reported compressibility data for methane (1) to obtain the three parameters K_o, v_0 , and v_1. Then, the hard sphere (monomer) excluded volume, b, was obtained from

$$b = B + (2RT)K_o \qquad (9)$$

Two functional forms found useful for regressing K_o and b versus temperature are as follows

$$\ln K_o = I + S(10^3/T) \qquad (10)$$

wherein S and I are constants, and

$$b = b_o + b_1 \exp(-C/T) \qquad (11)$$

wherein b_o and b_1 are constants. The temperature dependence of the two excluded volume parameters v_o and v_1 was considered to be linear with temperature in the range of temperatures involved in this work.

DATA FITTING PROCEDURE

The P-V-T data for methane were taken from compiled and edited IUPAC tables (1) which provided smoothed values for the second virial coefficient B versus temperature from 95 K to 620 K and the compression factor Z over the same range of temperature and extended ranges of pressure (as well as other useful P-V-T properties of methane). The temperature range used in this development was selected to include pressure values to 1000 MPa. The compression factor values up to 1000 MPa were limited to temperatures up to and including 470 K. It was felt that a 110 degree range of temperatures was sufficient to test the behavior of the essential fitting equation (8).

The smoothed tabled compression factor values and the corresponding second virial coefficient at each temperature versus pressure were used to establish the three coefficients in equation (8). SigmaPlot software was used to accomplish the regressions. A Marquardt-

Levenberg algorithm (2) was employed by the fitting program for the regressions. For every isotherm studied, convergence was rapid and in no case were more that twenty cycles required for generation of the coefficients.

Once the K_o values were established, the hard sphere volumes, b, could be obtained from equation (9) using the tabled second virial coefficient values. The variation of b with temperature provided the basis for the fitting equation (11) which provided estimates for b at temperatures below the temperature range studied. Once the b value estimates were obtained for the lower temperatures, the equation (9) along with tabulated second virial coefficients could be used to establish K_o value estimates for the lower temperature range. This technique was not extended to temperatures much above the temperature range of this study, 360-470 K, because of the uncertainty of the b values in the higher temperature range.

CALCULATED PARAMETERS AND RESULTS

Table 1 lists the K_o, b, v_o, and v_1 values obtained from equations (8) and (9) by regression procedures. The values are recorded without complete roundoff for significance to facilitate their use in further smoothing calculations. (Error estimates were provided by the interation software for each of the calculated parameters.)

TABLE 1. Calculated K_o, b, v_o, and $-v_1$ values from equations (8) and (9).

T /K	$K_o x 10^3$ /MPa^{-1}	b /cm^3/mol	v_o /cm^3/mol	$-v_1$ /cm^3/mol
360	7.706	22.93034	92.490	37.948
370	7.139	23.02712	95.305	45.457
380	6.627	23.15491	97.614	52.471
390	6.170	23.31690	99.490	59.041
400	5.756	23.51254	100.841	65.116
410	5.385	23.74527	101.905	70.899
420	5.051	24.01370	102.534	76.256
430	4.749	24.31608	102.805	81.229
440	4.479	24.64986	102.765	85.842
450	4.235	25.01427	102.419	90.112
460	4.014	25.40231	101.893	94.119
470	3.814	26.59332	101.065	97.734

Table 2 lists the reported second virial coefficient values over the extended temperature range in and below the range of this study, the b values from equation (11), the calculated K_o values from equation (9), and corresponding $-\ln(K_o)$ values, all in the same temperature range.

The recorded values found in Tables 1 and 2 provided the basis for the construction of all subsequent figures. Figure 1 shows the observed and calculated behavior of the function (Z - BP) = f(P). The observed values were obtained from the tabled B and Z versus P values of reference (1). Regressions were done at ten unit intervals of temperature; however, the figure only shows every other isotherm calculated for clarity.

TABLE 2. Calculated b, K_0 and $-\ln(K_0)$ together with second virial coefficients from reference (1).

T /K	B[a] /cm³/mol	b[b] /cm³/mol	$K_0 \times 10^3$ /MPa^{-1}	$-\ln(K_0)$
95	-456.7	21.9291	303.0	1.19408
100	-406.7	21.9291	257.8	1.35570
125	-252.9	21.9291	132.2	2.02329
150	-176.2	21.9292	79.43	2.53284
175	-130.9	21.9297	52.52	2.94659
200	-100.9	21.9323	36.93	3.29862
250	-63.4	21.9677	20.54	3.88562
300	-40.7	22.1309	12.59	4.37446
350	-25.5	22.5870	8.26	4.79605
400	-14.7	23.5254	5.75	5.15909
450	-6.6	25.1097	4.24	5.46375
500	-0.4	27.4502	3.35	5.69889
550	4.4	30.5986	2.86	5.85537
600	8.3	34.5562	2.63	5.94015
620	9.6	36.3586	2.60	5.95399

[a] Values from reference (1), pp. 54-55.
[b] Calculated from [11] using b_0 = 21.9291, b_1 = 790.12, and C = 2481.8.

The observed (smoothed) values are represented as points and the calculated values are shown as lines. Figure 2 shows the calculated deviations from the regressions shown in Fig. 1. The regression procedure (2) assigned equal weight to all data points along each isotherm. The deviations show a regular oscillating pattern for all isotherms which suggests a consistency of the data in the pressure and temperature ranges investigated.

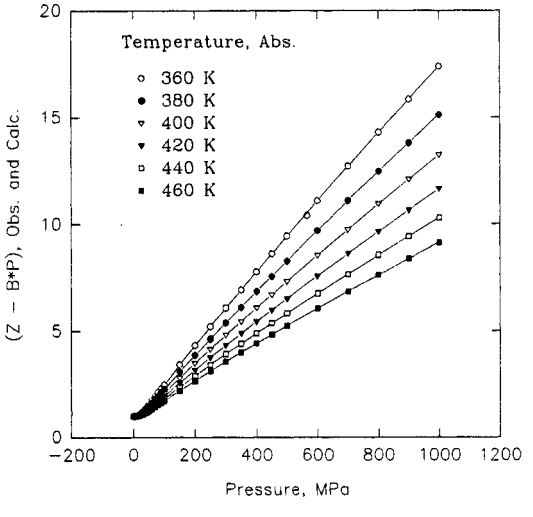

Fig. 1 (Z - BP) observed and calculated behavior, 360-470 K, 0-1000 MPa.

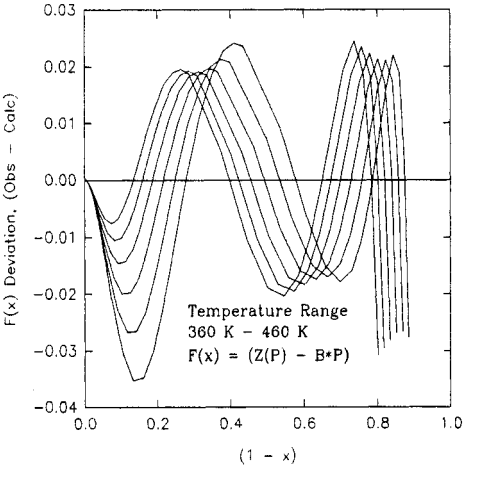

Fig. 2 Calculated deviations from the least square regression.

Additionally, the deviations appear to be well within the reported uncertainties for the tabulated data used in the regression procedure and the relative deviations all decrease with increasing pressure throughout the pressure range involved.

Figure 3 shows the temperature dependence of $\ln(K_o)$ and $\ln(b/RT)$ as functions of reciprocal absolute temperature. The linearity appears reasonable. However, the correlations with the second virial coefficient, as expressed in equation (9), beyond the temperature range considered indicates a nonlinear behavior of the two relations shown in Fig. 3. Figure 4 shows the calculated b values in the 360-460 K temperature range from equation (9), as open circles A, along with the reported liquid molar volumes from (1) along the equilibrium saturation liquid-vapor curve, as open circles B. Also shown as a

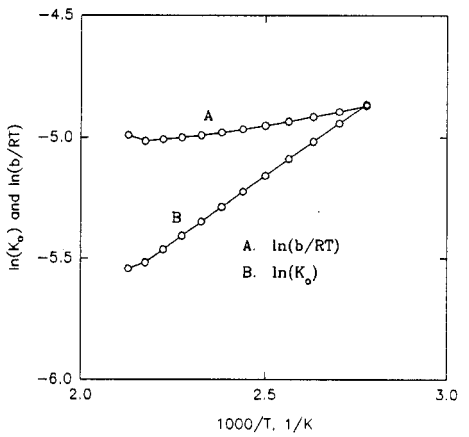

Fig. 3 Temperature dependence of $\ln(K_o)$ and $\ln(b/RT)$, 360-470 K.

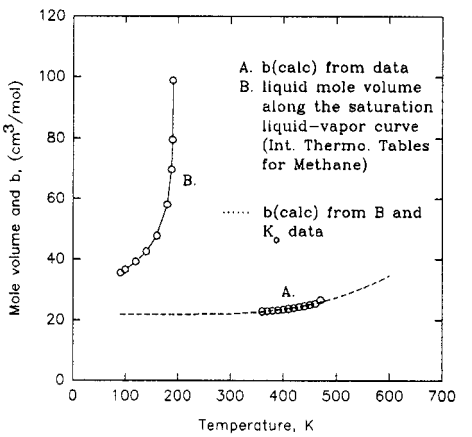

Fig. 4 Calculated b and liquid molar volumes along the saturation liquid-vapor curve.

dashed line are b values calculated from equation (11). One should expect the b values to be less than the liquid molar volume throughout the liquid phase region. The behavior shown in Fig. 4 appears to support this argument.

Figure 5 shows the calculated $\ln(K_o)$ values versus the reciprocal of absolute temperature both from the regression of the reported data using equation (8), as open

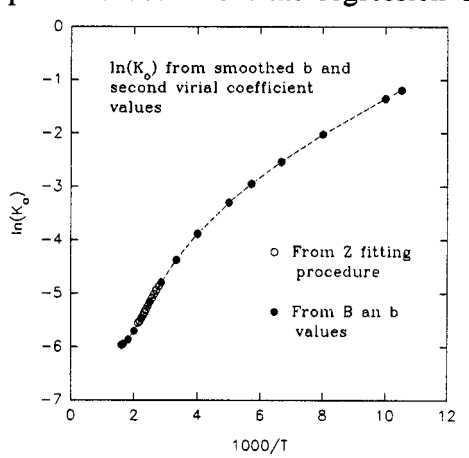

Fig. 5 Calculated $\ln(K_o)$ from Z, b, and second virial coefficients.

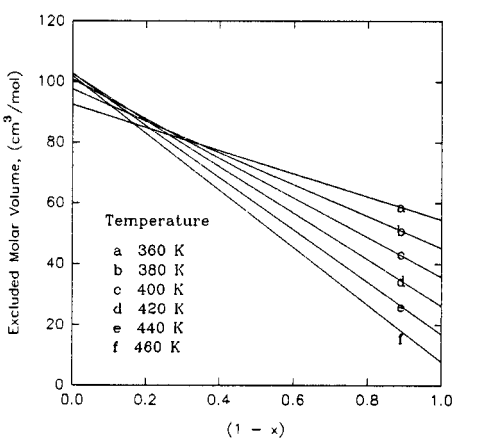

Fig. 6 Excluded molar volume V_e versus total associated species mole fraction.

circles, and from equation (9) using reported B values and the b values obtained from

equation (11), as solid circles. Figure 6 shows the excluded molar volume V_c versus the total associated complex mole fraction over the temperature range 360-460 K.

Figure 7 shows the actual excluded volume of the associated cluster species V_c versus total associated species mole fraction (1 - x), taking into account (n_c/n_o) versus

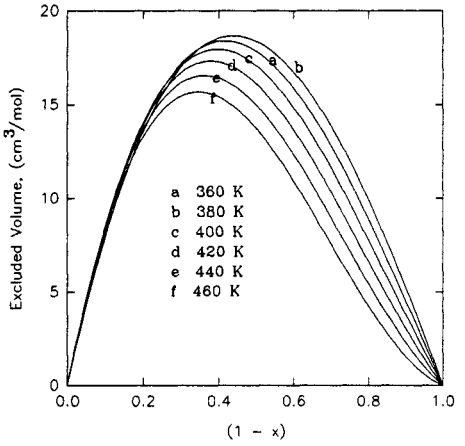

Fig. 7 Associated species excluded molar volume versus total associated complex species mole fraction, 360-460 K.

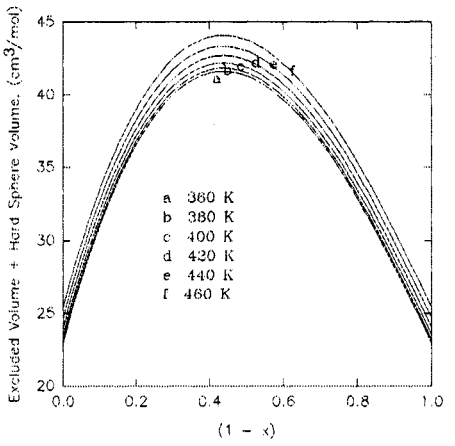

Fig. 8 V_c plus the hard sphere volume b versus total associated complex mole fraction, 360-460 K.

pressure. Values were obtained from V_c, as given by equation (7) and shown in Fig. 6, and (n_c/n_o) versus pressure as given in equations (3) and (8). Figure 8 shows V_c plus the hard sphere volume b versus (1 - x) which represents all system volume not included in the free volume of the monomer point masses. The behavior shown in Fig. 7 and Fig. 8 is quite reasonable considering the moles of associated species increase with increasing

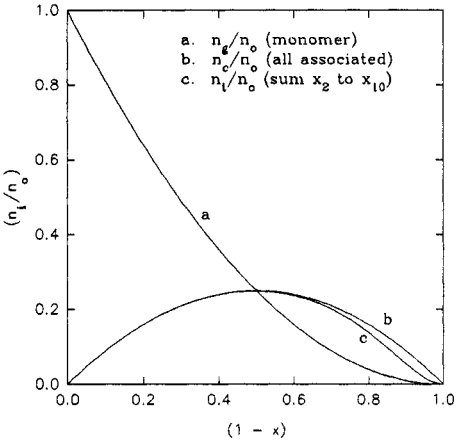

Fig. 9 Mole ratios (n_i/n_o) for monomer, total associated species, and sum of dimer through decimer species versus (1 - x).

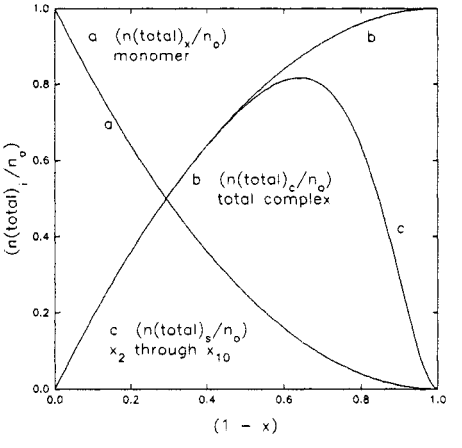

Fig. 10 Ratio total monomer moles in associated specie i to total monomer moles versus (1 - x).

pressure, beginning at low pressures, then, as the sizes of the associated species becomes larger, the total moles of associated species relative to n_o passes through a maximum and

then decreases, going to zero, as the pressure goes to infinity and (1 - x) goes to one.

Figure 9 shows the behavior of the ratio (n_i/n_o) versus total associated complex species mole fraction. Curves are shown for the monomer (a), the total associated species (b), and the dimer through decimer associated species (c). Figure 10 shows the distributions among species of the stoichiometric monomer moles n_o versus total associated complex species mole fraction. Both Fig. 9 and Fig. 10 show the increased involvement of the higher associated species, larger than the decimers, only beyond (1 - x) = 0.5. However, Fig. 10 shows more clearly the actual distribution of stoichiometric monomer moles among the associated species. The associated species exceed, on a mole basis, the moles of monomer in the system at (1 - x) = 0.5 as seen in Fig. 9 and, on the basis of the distribution of stoichiometric moles, n_o, unassociated monomer moles relative to associated monomer moles drops below 0.5 in the 0.3 range of (1 - x) as seen in Fig. 10.

SUMMARY OF OBSERVATIONS AND CONCLUSIONS

A model for supercritical fluid solvent P-V-T behavior based upon multiple associations and cluster formations and incorporating a cluster excluded volume parameter in addition to a hard sphere volume has been developed. The model provides a satisfactory means for describing supercritical fluid P-V-T behavior over a wide range of supercritical conditions with relatively few equation of state parameters. Good agreement has been obtained with the model for methane as a test system in the supercritical P-V-T region 360-470K and 0-1000 MPa.

The model suggests that the monomer specie can be assumed to account for the free volume behavior of a fluid over wide ranges of pressure and temperature conditions even at extremely high pressures far above the supercritical region. It can also be argued that the association clusters must exchange energy primarily through vibrational and rotational motions rather than translations which involve the free volume of the system. The model demonstrates a smooth transition of species from the monomer at low pressures to the predominately highly clustered species at high pressures.

A serious shortcoming of this cluster model is the fact that, in the absence of an internal pressure term, it cannot show phase separation phenomena. However, the incorporation of appropriate internal pressure terms should provide a satisfactory remedy for this problem. Most certainly, manifestations of internal pressures as may arise from surface tension forces associated with the cluster species should become significant somewhat above and in the critical region of a fluid.

REFERENCES

1. S. Angus, B. Armstrong and K.M. de Reuck. *International Thermodynamic Tables of the Fluid State-5 Methane* **IUPAC Chemical Data Series No. 17**, pp. 58-187, Pergamon Press, New York, N.Y. (1978).

2. *SigmaPlot Transforms and Curve Fitting Reference*, application of the Marquardt-Levenberg algorithm, chapter 7, Jandel Scientific, San Rafael, Calif. (1992).